# Chapter 2
# Neutrino Oscillation

*Physics works, and I'm still alive.*
Walter Lewin

## 2.1 Neutrinos and the Standard Model of Particle Physics

The Standard Model ($\mathscr{SM}$) of particle physics is the theory describing how the fundamental constituents of our universe interact. From the technical point of view the $\mathscr{SM}$ is a re-normalisable gauge field theory, based on the symmetry group $SU(3)_C \bigotimes SU(2)_L \bigotimes U(1)_Y$ which describes the strong, weak and electromagnetic interaction, via the exchange of spin-1 gauge field: eight massless gluons for the strong interaction, one massless photon for the electromagnetic interaction and three massive bosons, $W^{\pm}$ and $Z^0$ for the weak interaction.

The known elementary particles and antiparticles are fermions with spin-$\frac{1}{2}$ and are organised in two families according on how they interact: quarks and leptons. Quarks interacts with all the three forces, while leptons interact only through the electromagnetic and/or the weak force. Quarks and leptons exist in three generations or flavours, with different masses and flavour quantum numbers, but with identical interactions, which make the $\mathscr{SM}$ symmetric with respect to the flavour. A summary of $\mathscr{SM}$ fermions and bosons is shown in Fig. 2.1.

The fermions are a representation of the symmetry group and can be written as:

$$\begin{pmatrix} \nu_l \\ l^- \end{pmatrix}_L, \begin{pmatrix} q_u \\ q_d \end{pmatrix}_L, \; l_R^-, \; q_{uR}, \; q_{dR}, \tag{2.1}$$

where the left-handed fields are $SU(2)_L$ doublet, while the right handed fields are $SU(2)_R$ singlets. Neutrinos interact only via the weak force and they are experimentally observed with left-handed helicity, thus a right-handed neutrino is not included in the $\mathscr{SM}$.

© Springer Japan 2015

T. Junqueira de Castro Bezerra, *Double Chooz and Reactor Neutrino Oscillation*,
Springer Theses, DOI 10.1007/978-4-431-55375-5_2

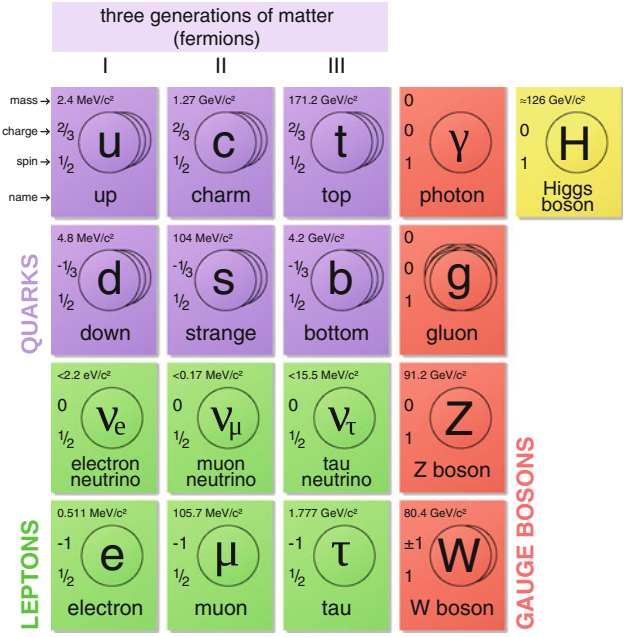


**Fig. 2.1** Fermions and Bosons described by the Standard Model of elementary particles. For each fermion (three generations of matter) there is an antiparticle, which are not shown for brevity. The gauge bosons are in the fourth column and the Higgs boson in the fifth. *Source* Creative Commons

Due to the gauge symmetry of the theory, particles are so far massless. While such assumption appears as a good approximation at high energies ($E \gg M_Z, M_W$), where the weak and electromagnetic interactions have similar strengths and are described by the unique electroweak force, at low energies the mass of the $W^{\pm}$ and Z bosons make the weak interaction weaker than the electromagnetic interaction.

The weak gauge bosons masses are acquired by introducing a new scalar field and breaking the gauge symmetry by choosing an expectation value for its vacuum state. This mechanism, known as spontaneous symmetry breaking, generates the masses for the weak bosons and give rise to the appearance of the spin-0 Higgs boson. The photon and the gluons remain, by construction, massless particles in agreement with experimental observations.

Once the gauge symmetry is broken, also fermions are allowed to acquire a mass term through the so called Higgs mechanism which couples the right-handed singlets with the left-handed doublets via the Yukawa coupling constant, providing masses of the form of

$$\mathscr{L}_Y = m_l \bar{l}_L l_R + m_q \bar{q}_L q_R + h.c., \tag{2.2}$$

where the mass term for the fermions (for example) is given by $m_l$:

$$m_l = \frac{v}{\sqrt{2}} \Gamma_l, \tag{2.3}$$

where $v$ is the vacuum expectation value of the Higgs field and $\Gamma_l$ is the Yukawa coupling constant, that assumes different values for the different fermions. To explain the observed masses, $\Gamma_l$ varies from $\sim$1 for the heaviest fermion, the top quark, to $\sim 10^{-5}$ for the lighter charger fermion, the electron.

Since the observed neutrinos are only left-handed, they are not allowed to acquire mass though the Higgs mechanism, remaining massless in the $\mathscr{SM}$. The $\mathscr{SM}$ provides a beautiful theoretical model which is able to accommodate most of the present knowledge on electroweak and strong interactions. It is able to explain many experimental facts and, in some cases, it has successfully passed very precise tests. Even the long search for the Higgs boson has recently provided conclusive evidence for the discovery of a new particle, consistent with the $\mathscr{SM}$ Higgs boson hypothesis [1].

In spite of the impressive phenomenological success, the $\mathscr{SM}$ leaves many unanswered questions to be considered as a complete description of the fundamental forces. There is no understanding regarding the existence of three (and only three) fermions families as well as their origins. There is no answer to the observed mass spectrum and mixing pattern. These, and others questions remain open and require new physics beyond the $\mathscr{SM}$. As will be stressed in the rest of this chapter, the first hint from such new physics has emerged with evidence of neutrino oscillations.

## 2.2 Neutrino Oscillation Theory

Neutrino oscillation were postulated in 1957 by Pontecorvo [2]. In analogy with $K^0 \leftrightarrow \bar{K}^0$ oscillations, Pontecorvo suggested the possibility of neutrino-antineutrino oscillation ($\nu \leftrightarrow \bar{\nu}$). When the second neutrino family where discovered, Maki, Nakagawa and Sakata proposed in 1962 the possibility of oscillation among the neutrino families introducing the concept of lepton flavour mixing [3]. The neutrino oscillation mechanism is based on the fact that if neutrinos have a non-zero mass, flavour states $|\nu_\alpha\rangle$ (interaction states) and mass states $|\nu_i\rangle$ (propagation states) could not coincide, in analogy to the mixing in the quark sector, i.e.,

$$|\nu_\alpha\rangle = \sum_i U^*_{\alpha,i} \, |\nu_i\rangle \, , \tag{2.4}$$

where $\alpha$ represent the flavour families ($e$, $\mu$, $\tau$), $|\nu_i\rangle$ the mass states of mass $m_i$ (with i = 1, 2, 3) and $U$ is the so called PMNS (Pontecorvo-Maki-Nakagawa-Sakata) unitary mixing matrix. Neutrinos are produced via weak interaction in a defined flavour eigenstate $|\nu_\alpha\rangle$ together with the corresponding lepton $\alpha$. For a neutrino produced at time $t = 0$, $|\nu\rangle\,(t = 0) = |\nu_\alpha\rangle$, and propagating it as a free particle

following the Schrödinger equation, after a time $t$ and travelled distance $L$, it will be described by

$$|\nu_\alpha(t, L)\rangle = \sum_i U^*_{\alpha,i} e^{-i(E_i t - pL)} |\nu_i\rangle , \tag{2.5}$$

where $E$ and $p$ is the neutrino energy and momentum, respectively. Assuming the three mass eigenstates propagate with the same momentum with relativistic energies ($p \simeq E \gg m_i$):

$$E_i = \sqrt{p^2 + m_i^2} \simeq p + \frac{m_i^2}{2p} \simeq E + \frac{m_i^2}{2E}. \tag{2.6}$$

Thus, Eq. 2.5 can be re-written, using natural units ($c = \hbar = 1$), as

$$|\nu_\alpha(t, L)\rangle = \sum_i U^*_{\alpha,i} e^{-i\frac{m_i^2}{2E}L} |\nu_i\rangle . \tag{2.7}$$

In other words, the initial mass state components evolve independently acquiring phases depending from their masses. Equivalently, Eq. 2.7 can be reverted to express the mass eigenstate $|\nu_i\rangle$ as a function of the flavour eigenstate $|\nu_\beta\rangle$,

$$|\nu_i(L)\rangle = \sum_{\beta=e,\mu,\tau} \left( \sum_i U^*_{\alpha,i} e^{-i\frac{m_i^2}{2E}L} U_{\beta,i} \right) |\nu_\alpha\rangle . \tag{2.8}$$

A neutrino created at $t = L = 0$, with $\alpha$ flavour state, evolves as a linear superposition of the existing lepton states. Like the production, the detection of neutrinos occurs via the weak interaction. The probability to observe a neutrino created with flavour $\alpha$, at $L = 0$, with a different flavour $\beta$, after a distance $L$, is defined as

$$\begin{aligned} P\left(\nu_\alpha \to \nu_\beta\right) &= \left|\langle \nu_\beta | \nu_\alpha(L) \rangle\right|^2 = \left| \sum_i U^*_{\alpha,i} U_{\beta,i} e^{-i\frac{m_i^2}{2E}L} \right|^2 \\ &= \sum_i \left| U_{\alpha,i} U^*_{\beta,i} \right|^2 + 2Re \left( \sum_{i>j} U_{\alpha,i} U^*_{\beta,i} U^*_{\alpha,j} U_{\beta,j} e^{-i\frac{\Delta m_{ij}^2}{2E}L} \right) . \end{aligned} \tag{2.9}$$

In the equation above an oscillation term appears as a function of the distance between the neutrino creation point (source) and the detection point (detector), and the neutrino energy. The oscillation frequency is proportional to the squared difference between the mass states, $\Delta m_{ij}^2 = m_j^2 - m_i^2$, while the oscillation amplitude is proportional to the PMNS matrix elements, $U_{\alpha,i}$.

The PMNS matrix is defined as

$$U = \begin{pmatrix} c_{12}c_{13} & s_{12}c_{13} & s_{13}e^{-i\delta} \\ -s_{12}c_{23} - c_{12}s_{23}s_{13}e^{i\delta} & c_{12}c_{23} - s_{12}s_{23}s_{13}e^{i\delta} & s_{23}c_{13} \\ s_{12}s_{23} - c_{12}s_{23}s_{13}e^{i\delta} & -c_{12}s_{23} - s_{12}c_{23}s_{13}e^{i\delta} & c_{23}c_{13} \end{pmatrix}, \tag{2.10}$$

where $c_{ij} = \cos\theta_{ij}$ and $s_{ij} = \sin\theta_{ij}$. The angles $\theta_{12}$, $\theta_{13}$ and $\theta_{23}$ represent the mixing angles and $\delta$ is a CP violation phase. Two additional phases have to be taken into account if neutrinos are Majorana particles, but such phases do not impact the neutrino oscillation.

As shown in Eq. 2.9, neutrino oscillations depend also on the mass squared differences between the mass states, namely $\Delta m^2_{21}$, $\Delta m^2_{32}$ and $\Delta m^2_{31}$, which only two of them are independent, since there is the relation

$$\Delta m^2_{31} = \Delta m^2_{32} + \Delta m^2_{21}. \tag{2.11}$$

Consequently, neutrino oscillation depends on six free parameters: three mixing angles, two mass squared differences and one complex CP violation phase. For practical reasons, the mixing matrix is usually factorized in terms of three matrices $M_{2,3} \times M_{1,3} \times M_{1,2}$ as

$$U = \begin{pmatrix} 1 & 0 & 0 \\ 0 & c_{23} & s_{23} \\ 0 & -s_{23} & c_{23} \end{pmatrix} \begin{pmatrix} c_{13} & 0 & s_{13}e^{-i\delta} \\ 0 & 1 & 0 \\ -s_{13}e^{i\delta} & 0 & c_{13} \end{pmatrix} \begin{pmatrix} c_{12} & s_{12} & 0 \\ -s_{12} & c_{12} & 0 \\ 0 & 0 & 1 \end{pmatrix}. \tag{2.12}$$

As one can see, each matrix is related to a different mixing angle. $M_{2,3}$ is parametrized in terms of $\theta_{23}$ which is the mixing angle dominating the $\nu_\mu \rightarrow \nu_\tau$, related to the oscillation of atmospheric and accelerator neutrino. $M_{1,2}$ is parametrized in terms of $\theta_{12}$ dominating the transition $\nu_e \rightarrow \nu_{\mu,\tau}$, related to the oscillation of neutrino coming from the sun and long baseline reactors. Finally, $M_{1,3}$ depends on $\theta_{13}$ which is the mixing matrix dominating the oscillation $\nu_\mu \rightarrow \nu_e$, and short baseline reactor $\bar{\nu}_e \rightarrow \bar{\nu}_e$. The CP phase always appears multiplied by the terms $\sin\theta_{12} \sin\theta_{23} \sin\theta_{13}$, so it would be measurable only if $\theta_{13}$ is different than zero.[1]

Finally, the observation of the neutrino oscillations has two main consequences: neutrinos have a non-zero mass and the lepton flavour is not conserved.

## 2.3 Matter Effects

When discussing oscillation searches where the neutrino beam passes through a portion of the Earth, one must consider the influence of matter on neutrino propagation. During propagation, electron neutrinos and antineutrinos may forward-scatter via charged current interactions with electrons in the surrounding matter medium. This

[1] Some experiments showed non zero value for the other two angles, as it is showed in next sections.

phenomena was first considered by Mikheyev and Smirnov [4], and Wolfenstein [5], and is now known as the MSW effect. While most neutrinos observed in experiments pass through part of the Earth at some point, it has been shown by De Rújula [6] that matter effects only impact experiments with a baseline in the order of 1,000 km. Thus, while this effect has little impact on experiments where $L \sim 1$ km, as in reactor neutrino experiments, it does need to be considered in accelerator based neutrino experiments searching for neutrino appearance at long baselines.

Any area of electron density $N_\alpha$ can be considered to contribute an effective potential term to the flavor basis Hamiltonian $V_\alpha = \sqrt{2} G_F N_\alpha$, where $G_F$ is the Fermi constant. Since the Earth presents a density of only electrons, $V = (\sqrt{2} G_F N_e, 0, 0)$. Neutral current scattering contributes a term which is equal for all flavour eigenstates, and thus a negligible multiple of the identity matrix. The MSW effect will modify the oscillation probability, defined in Eq. 2.9, as proposed in [7].

Depending on the experimental parameters, matter effects can mimic a CP-violating signal. This effect also depends on the ordering of the neutrino masses, or the mass hierarchy. Since the absolute hierarchy has not yet been established, this variable can affect experiments sensitivity on measuring $\delta_{CP}$.

The Sun is a pure source of $\nu_e$, as described in Sect. 2.5.1.1. In analogy to neutrinos travelling through the Earth, solar neutrinos oscillations have to account for the matter effects. However, in the Sun, the electron density $N_\alpha$ changes as a function of the radius. If the evolution of the propagation Hamiltonian is adiabatic, then $\nu_e$ produced in the Sun's interior will evolve into $\nu_2$, which is defined such that $\nu_2 > \nu_1$. Evidence suggests that $>90\,\%$ of $^8$B's $\nu_e$ produced in the Sun's core evolve into $\nu_2$ due to matter effects [8]. Therefore, to a first approximation, the $\nu_e$ flavour content of $^8$B solar neutrinos reach the Earth is expected to be $|U_{e2}| \sim \sin^2 \theta_{12}$.

## 2.4 Mass Hierarchy

In the full three flavour model of neutrino mixing, a hybrid approach to labelling the neutrino mass eigenstates is taken. The mass squared splittings are known to be hierarchical, therefore it is possible to define $\nu_3$ as the neutrino mass eigenstate whose mass is very different from the masses of the other two mass eigenstates (either much larger or much smaller), i.e., $|\Delta m^2_{21}| \ll |\Delta m^2_{32}| \sim |\Delta m^2_{31}|$. However, this definition does not specify the mass hierarchy, i.e., whether $m_3 > m_{1,2}$ or $m_3 < m_{1,2}$. Therefore, the sign of $\Delta m^2_{31}$ and $\Delta m^2_{21}$ can be either positive or negative. If $\Delta m^2_{31} > 0$, this is called the "normal" mass hierarchy. If however, $\Delta m^2_{31} < 0$, this is called the "inverted" mass hierarchy, as shown in Fig. 2.2. Matter effects from accelerator neutrino beams passing through the earth can be used to determine the mass hierarchy. The $m^2_2 > m^2_1$ hierarchy, was solved by the solar neutrino experiments, described in Sect. 2.5.1.1.

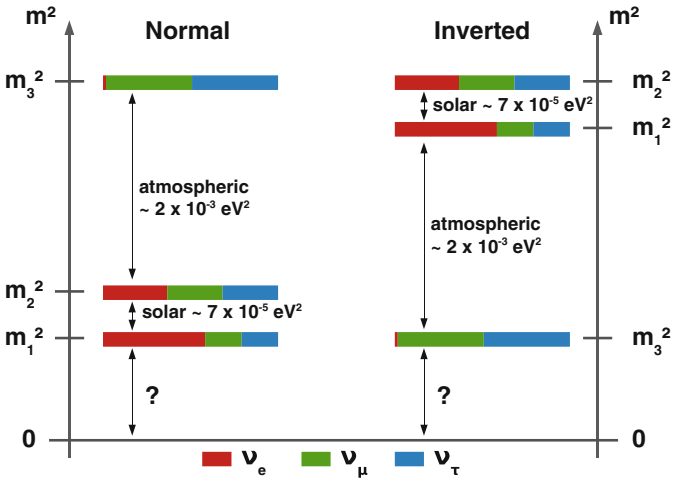


**Fig. 2.2** Neutrino mass eigenstates spectra for both cases of normal or inverted hierarchy, and composition in terms of $\nu_e$, $\nu_\mu$, and $\nu_\tau$. Neither the absolute scale, nor the 3-2 hierarchy arrangement are known so far

## 2.5 Measuring Neutrino Oscillation Parameters

To easily understand neutrino oscillation experimental results, the simplified case for two active neutrino is considered. The mixing between two neutrino families is described by a real and orthogonal $2 \times 2$ matrix with one mixing parameter, the rotation angle $\theta$ between the flavour and the mass eigenstates:

$$\begin{pmatrix} \nu_\alpha \\ \nu_\beta \end{pmatrix} = \begin{pmatrix} \cos\theta & \sin\theta \\ -\sin\theta & \cos\theta \end{pmatrix} \begin{pmatrix} \nu_1 \\ \nu_2 \end{pmatrix}, \tag{2.13}$$

and the oscillation probability takes the form

$$P(\nu_\alpha \to \nu_\beta) = \sin^2 2\theta \sin^2 \left( \frac{\Delta m^2 L}{4E} \right). \tag{2.14}$$

The oscillation amplitude, $\sin^2 2\theta$, is determined by the mixing angle $\theta$ and does not allow to distinguish between $\theta$ and $\pi/2 - \theta$, which are not physically equivalent.

Restoring to physics units, the oscillation phase, $\phi$, becomes

$$\phi = 1.27 \left( \frac{\Delta m^2[\mathrm{eV}^2] L[\mathrm{km}]}{E[\mathrm{GeV}]} \right). \tag{2.15}$$

In the limit where $\phi \ll 1$, $P(\nu_\alpha \to \nu_\beta) \simeq \sin^2 2\theta (\Delta m^2 L/4E)^2$, so the measurement of the oscillation probability would determine information only on the product

$\sin^2 2\theta \times \Delta m^2$. The oscillation would not have enough time to develop and the number of neutrino oscillation events measured in the detector is approximately independent from the distance $L$, since the oscillation goes with $(L/E)^2$ and the neutrino flux diminish with $1/L^2$.

In the opposite where $\phi \gg 1$, the oscillation are so fast that get averaged out, $P(\nu_\alpha \to \nu_\beta) \simeq 1/2 \sin^2 2\theta$. In this limit the oscillation probability does not depend from the oscillation phase and the number of events decrease with $1/L^2$.

In order to measure both oscillation parameters, the measurement of the averaged probability is not enough, and the $L$ (or $E$) dependence must also be measured to characterise the oscillation pattern. Thus, a good possible experimental condition to characterise oscillation parameters is then to have an oscillation phase of $\simeq 1$.

Even if three neutrino families exist, the mixing parameters are such that the dominant oscillation pattern is driven by the two flavour mixing, while the third flavour contribute at the second or higher order. For this reason the results of oscillation experiments are often shown in a two neutrino scenario and determine a single mixing angle and squared mass difference.

### 2.5.1 Measurement of $\Delta m^2_{21}$ and $\theta_{12}$

Measurement of $\Delta m^2_{21}$ and $\theta_{12}$ oscillation parameters has been performed by the experiments detecting $\nu_e$ produced by the Sun's thermonuclear reactions and non-natural terrestrial $\bar{\nu}_e$ source, such as nuclear reactors.

#### 2.5.1.1 By Solar Neutrinos

Solar neutrinos are $\nu_e$ produced by the reactions responsible for solar energy production, such as $4p + 2e^- \to {}^4\mathrm{He} + 2\nu_e + 26.7\,\mathrm{MeV}$. This process takes place through different nuclear reactions and consequently solar neutrinos are characterised by different energy spectra as shown in Fig. 2.3. The typical neutrino flux reaching the Earth is of about $10^{12}\ \nu/\mathrm{s/cm^2}$. Several experiments measured the solar neutrino flux, starting in 1970 with the pioneering Chlorine experiment in the Homestake mine, proposed by Davis Jr. [10]. The $\nu_e$ flux were measured in a tank of $380\,\mathrm{m}^3$ filled with $C_2Cl_4$, placed 1,478 m underground, counting the number of radioactive ${}^{37}\mathrm{Ar}$ nuclei produced by the inverse beta decay reaction ${}^{37}\mathrm{Cl} + \nu_e \to {}^{37}\mathrm{Ar} + e^-$, which has a threshold energy of 814 keV. Only one third of the neutrino flux predicted by the Standard Solar Model (SSM) were measured. Although this could be the first indication of neutrino oscillation ($\nu_e$ disappearance), at that time an error on the experimental measurements or in the SSM was assumed as possible explanation of the observed deficit.

Another type of radiochemical experiments (Gallex [11], GNO [12] and SAGE [13]), used ${}^{71}\mathrm{Ga}$ which interacts through the reaction ${}^{71}\mathrm{Ga} + \nu_e \to {}^{71}\mathrm{Ge} + e^-$

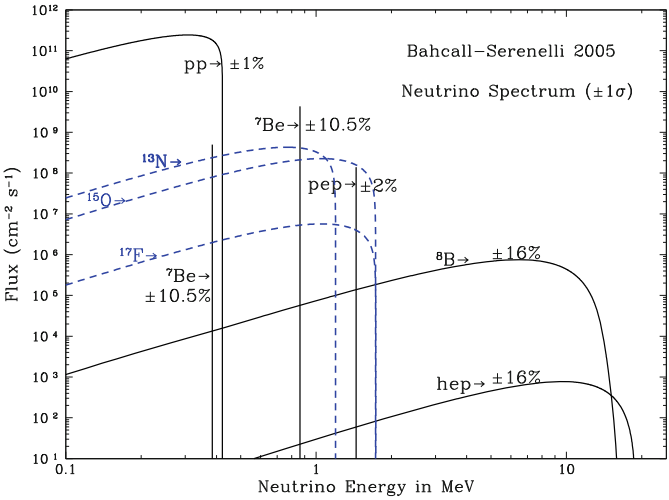


**Fig. 2.3** The solar neutrino energy spectrum of each SSM production process. Reprinted figure with permission from [9]

that has a threshold energy of 233 keV. Thus, the neutrinos from the pp-chain can be detected, and the solar neutrino flux can be known model independent. These experiments also found a deficit when comparing with the SSM prediction flux. The Super-Kamioka Neutrino Detection Experiment (Super-Kamiokande or simply SK) [14] measured the energy spectrum of solar $^8$B neutrinos. The observed spectrum was compared with the SSM prediction without oscillation, resulting in a poor agreement at 4.6 % confidence level. While all these experiments, performed with different techniques, confirmed the deficit in the solar neutrino flux, the theoretical model uncertainty were excluded by a better understanding of the Sun, and this deficit became the so called Solar Neutrino Anomaly.

The solar neutrino anomaly was only solved later by the Sudbury Neutrino Observatory (SNO) experiment [15, 16] using a heavy water ($D_2O$) Čerenkov detector, sensible to neutrino interactions through three different interaction processes:

- Elastic scattering (ES): $\nu_x + e^- \rightarrow \nu_x + e^-$ with $x = e, \mu, \tau$, involving all neutrino types but with a different cross-section for $\nu_\mu$ and $\nu_\tau$;
- Charged current (CC): $D + \nu_e \rightarrow 2p + e^-$, involving only electron neutrinos;
- Neutral current (NC): $D + \nu_x \rightarrow p + n + \nu_x$, involving all neutrino flavour with the same cross-section.

Naming $\phi_x$ the neutrino flux for the flavour $x$, ES allows to determine the flux $\phi_{ES} = \phi_e + 0.155(\phi_\mu + \phi_\tau)$, CC determines $\phi_{CC} = \phi_{\nu_e}$ and NC determines the total flux $\phi_{Tot.} = \phi_e + (\phi_\mu + \phi_\tau)$. Thus, the ratio of CC/NC can be interpreted as a ratio of $\nu_e$ flux to the total flux of the three flavours. The measured fluxes are:

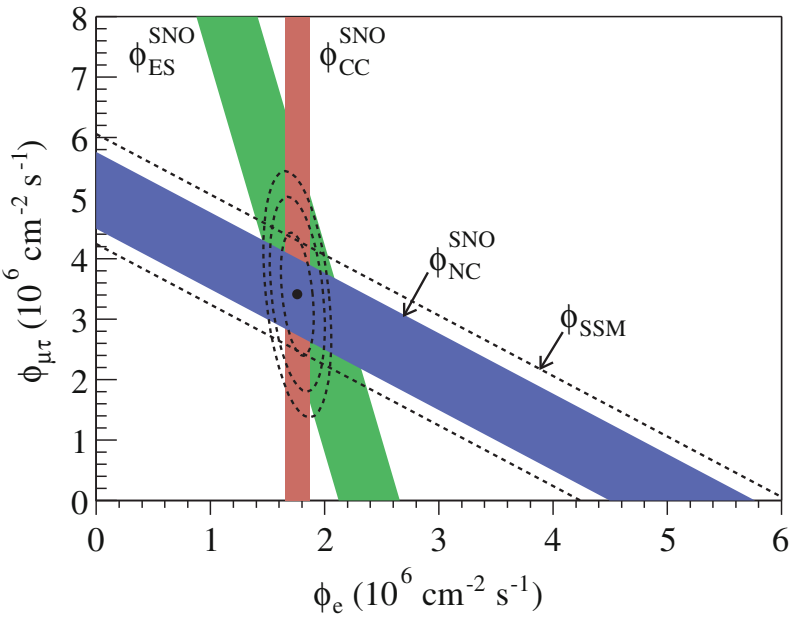


**Fig. 2.4** Flux of $^8$B solar neutrinos that are $\mu$ or $\tau$ flavour vs. flux of electron neutrinos deduced from the three neutrino reactions, ES, NC and CC, in SNO (1 $\sigma$ allowed region). The $^8$B expected flux from the SSM is also shown. The bands intersect at the fit values for $\phi_e$ and $\phi_{\mu\tau}$, indicating that the combined flux results are consistent with neutrino flavour transformation. Reprinted figure with permission from [16]

$$\phi_{\rm ES} = 2.35 \pm 0.22(\text{stat.}) \pm 0.15(\text{sys.}) \times 10^6\,\text{cm}^{-2}\text{s}^{-1}$$
$$\phi_{\rm CC} = 1.68 \pm 0.06(\text{stat.})^{+0.08}_{-0.09}(\text{sys.}) \times 10^6\,\text{cm}^{-2}\text{s}^{-1}$$
$$\phi_{\rm NC} = 4.94 \pm 0.21(\text{stat.})^{+0.38}_{-0.34}(\text{sys.}) \times 10^6\,\text{cm}^{-2}\text{s}^{-1}$$

These three different reactions measured three independent linear combination of electron, muon and tau neutrino fluxes, as shown in Fig. 2.4. Such measurement allowed to obtain clear evidence of solar neutrino transmutation in terms of $\nu_e \rightarrow \nu_{e,\mu,\tau}$, of which $\nu_e$ is only one third of the total. Moreover, the total initial $\nu_e$ flux has been determined independently from theoretical model. Finally, since $\nu_\mu$ or $\nu_\tau$ can not be generated in the SSM, the result of non-zero $\nu_\mu + \nu_\tau$ fluxes is a strong evidence of the neutrino oscillation.

#### 2.5.1.2 By Long Baseline Reactor Neutrinos

The Kamioka Liquid Scintillator Antineutrino Detector (KamLAND) experiment also played an important role in the determination of the solar oscillation parame-

ters [17]. The KamLAND experiment, a 1 kton liquid scintillator detector located at the Kamioka mine under 2,700 m.w.e (meters water equivalent), detected $\bar{\nu}_e$ emitted by several nuclear power plants in Japan. The neutrino energy is of the order of few MeV and the average distance between detector and reactors is of about 180 km (flux weighted baseline). Given the mass squared difference measured by solar experiments of $\sim 7.5 \times 10^{-5}\,\text{eV}^2$, the oscillation phase, Eq. 2.15, is of the order of 1, which provides a good condition for a precise measurement of the oscillation parameters. The $\bar{\nu}_e$ detection is performed by the Inverse Beta Decay (IBD) process, described in details in Sect. 3.2, where the neutron is captured by the scintilaltor's Hydrogen nucleus.

Results of the KamLAND experiment show a significant spectral distortion in the final state positron energy spectrum, shown in the left plot of Fig. 2.5. The spectrum expected in non oscillation scenario is rejected with a significance better than 5 $\sigma$. The ratio of background subtracted $\bar{\nu}_e$ events to the non oscillation expectation is shown in the right plot of Fig. 2.5. In addition, due to the Great East Japan Earthquake of 2011, all the Japanese nuclear power plants were turned off for inspection, and the KamLAND collaboration could improve its result by a longer and more precise background measurement. This lead to a precise determination of the solar oscillation parameters of

$$\Delta m^2_{21} = 7.54^{+0.19}_{-0.18} \times 10^{-5}\,\text{eV}^2 \tag{2.16}$$

$$\tan^2\theta_{12} = 0.481^{+0.092}_{-0.080} \tag{2.17}$$

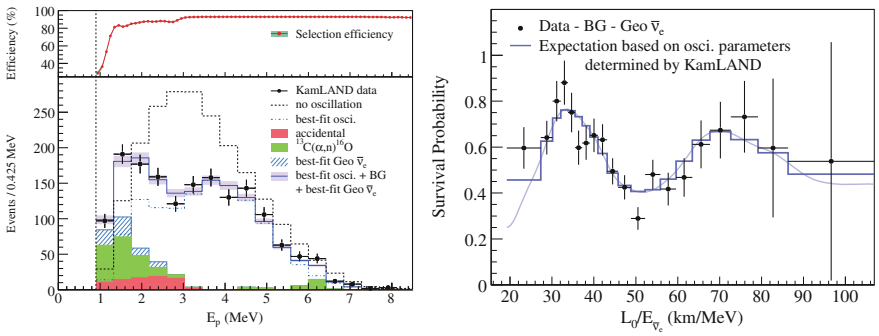


**Fig. 2.5** Energy spectrum and survival probability of $\bar{\nu}_e$ from the KamLAND experiment. On the *left* is the prompt event energy spectrum of $\bar{\nu}_e$ candidates corresponding to reactor spectra and expected backgrounds incorporating the energy dependent selection efficiency (*top panel*). On the *right* is the ratio of the background subtracted $\bar{\nu}_e$ spectrum to the expectation for non oscillation as a function of $L_0/E$, where $L_0$ is the effective baseline taken as a flux-weighted average ($L_0 \sim 180\,\text{km}$). Reprinted figure with permission from [17]

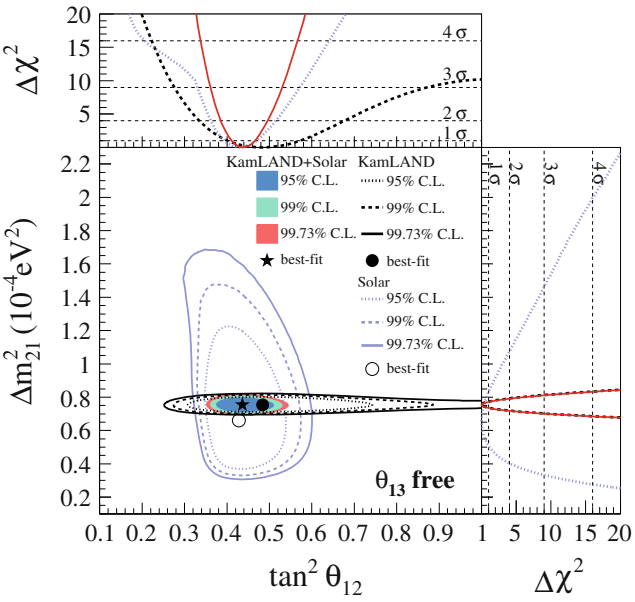


**Fig. 2.6** Allowed region for neutrino oscillation parameters from KamLAND and solar neutrino experiments. The side panels show the $\chi^2$ distribution for KamLAND (*dashed light blue line*) and solar experiments (*dotted black line*), as well as the combination of both (*solid red line*). Reprinted figure with permission from [18]

Results from a global three neutrino flavour oscillation analysis, combining both solar and KamLAND results without any constrain to $\theta_{13}$, are shown in Fig. 2.6, which gives the following best fit values,

$$\Delta m^2_{21} = 7.53^{+0.19}_{-0.18} \times 10^{-5}\ \text{eV}^2 \quad \text{and} \quad \tan^2\theta_{12} = 0.437^{+0.029}_{-0.026}, \tag{2.18}$$

and also $\sin^2\theta_{13} = 0.023 \pm 0.015$. These are the solar neutrino oscillation parameters measurements with the best precision so far.

### 2.5.2 Measurement of $\Delta m^2_{32}$ and $\theta_{23}$

The first measurement of $\Delta m^2_{32}$ and $\theta_{23}$ has been performed by SK using atmospheric neutrinos. Further measurements have been performed to confirm SK results by K2K, MINOS and Opera long baseline experiments, using $\nu_\mu$ produced by particle accelerators.

#### 2.5.2.1 By Atmospheric Neutrinos

Atmospheric neutrinos are produced by cosmic rays interacting in the high atmosphere producing mainly pions ($\pi^{\pm}$) and kaons (**K**). The majority of charged pions decay through the weak charged current $\pi^{\pm} \rightarrow \mu^{\pm}\nu_{\mu}(\bar{\nu}_{\mu})$. The muons subsequently decay as $\mu^{\pm} \rightarrow e^{\pm}\nu_e(\bar{\nu}_e)+\bar{\nu}_{\mu}(\nu_{\mu})$ giving, as a first approximation, two muon neutrinos for each electron neutrino. Their energy spans from a few MeV up to several GeV.

Atmospheric neutrinos observed at different zenith angles have various flight path lengths which vary from 10 to 30 km, for downward neutrinos, or up to $10^4$ km, for upward neutrinos, running through the Earth. Since neutrinos can be generated at any point of the atmosphere, neutrinos of the same energy can travel very different distances before reaching the detector, giving different oscillation probabilities. Thus a detector able to distinguish muon neutrinos from electron neutrinos and also able to recognise their incoming direction is necessary, and thus being sensitive for a wide range of $\Delta m^2$.

SK is a large water Čerenkov detector located in the Japanese Kamioka mine, under 2,700 m.w.e. depth to shield the detector from cosmic rays. It contains about 50 ktons of water and it is surrounded by about 13,000 PMTs. Neutrinos undergo charged current interaction producing charged leptons. The lepton is generally produced with relativistic energy and it is detected through the cone of Čerenkov light produced as it travels through the detector. The flavour of the lepton is identified by the sharpness of the Čerenkov ring. The position of the ring allows to determine the lepton direction, which is correlated to the neutrino direction for energies larger than $\sim$1 GeV. The lepton energy could also be obtained from the amount of light collected by the PMTs if the lepton stops into the detector. Even if the lepton energy is not strongly correlated to the neutrino energy it allows to handle the energy dependence of the oscillation probability. SK provided in 1998 the first firm evidence of neutrino flavour transition comparing the expected number of events with the observed ones, as a function of the zenith angle. SK observed that there are twice as many downward going $\nu_{\mu}$ than upward going $\nu_{\mu}$, as shown in the left plot of Fig. 2.7. The right plot shows the ratio between data and prediction at large $L/E$. The hypothesis that $\nu_{\mu}$ have interacted crossing the earth is not reliable because the earth is nearly transparent for neutrinos with energy of about few GeV and a similar behaviour should have also been found for $\nu_e$. Moreover, since no excess of the electron neutrino flux has been found, the observed oscillation is attributed to the transition $\nu_{\mu} \rightarrow \nu_{\tau}$. As a result from the oscillation fit [9], a 90 % confidence level region allows the following oscillation parameters

$$(1.9 < \Delta m^2_{32} < 3.0) \times 10^{-3}\ \text{eV}^2 \ \text{ and } \ \sin^2 2\theta_{23} > 0.90. \tag{2.19}$$

#### 2.5.2.2 By Accelerator Neutrinos

Long Baseline Neutrino Experiments use a muon neutrino beam from accelerators at energies of a few hundred MeV to a few GeV, produced by pion decay, where

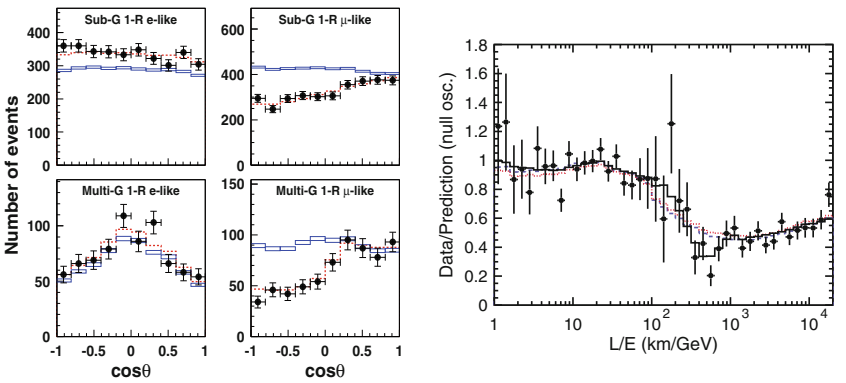


**Fig. 2.7** Results from SK phase I atmospheric neutrino data. The *left plot* shows the zenith angle distributions for fully contained 1-ring $e$-like and $\mu$-like events for sub-GeV and multi-GeV energies. Non oscillated MC events are represented by the *solid lines squares* and the *doted lines* represent the best fit expectation for $\nu_\mu \rightarrow \nu_\tau$ oscillations. The *right plot* shows the ratio between data and MC prediction without oscillation, as a function of the reconstructed $L/E$. The *solid line* represents the best fit in the two flavour oscillation scheme. Reprinted figures with permission from [19, 20]

the pions are generated from protons hitting on targets. These experiments have been performed to be an independent measurement of neutrino oscillation seen in atmospheric neutrino experiments. The oscillation parameters are measured through $\nu_\mu$ disappearance, $P(\nu_\mu \rightarrow \nu_\mu) = 1 - P(\nu_\mu \rightarrow \nu_x)$, in a detector hundreds of km far from the neutrino source.

The KEK to Kamioka (K2K) experiment in Japan used $\nu_\mu$ produced from a pulsed beam at The High Energy Accelerator Research Organization (KEK) and the 250 Km far away SK detector. The average neutrino energy is slightly above 1 GeV. Given the mass squared difference of about $2.5 \times 10^{-3}\,\text{eV}^2$ measured with atmospheric neutrino by SK, the oscillation phase is of the order of 1, which represent the best condition to measure oscillation. K2K compared the $\nu_\mu$ flux observed at SK with the non-oscillated flux measured by a 1 kton water Čerenkov detector placed at about 300 m from the neutrino source. K2K excluded the non oscillation with a confidence of 4.3 $\sigma$ and, in a two flavour oscillation scenario, the allowed $\Delta m^2$ region at $\sin^2 2\theta = 1$, with 90 % C.L., is

$$(1.9 < \Delta m^2_{32} < 3.5) \times 10^{-3}\,\text{eV}^2, \tag{2.20}$$

where the best fit value is $\Delta m^2_{32} = 2.8 \times 10^{-3}\,\text{eV}^2$ [21].

Another important experiment is the Main Injector Neutrino Oscillation Search (MINOS), placed in the Sudan mine, 735 km far from a neutrino pulsed beam produced at Fermilab. The neutrino energy, 1–5 GeV, is higher than K2K to obtain an oscillation phase of the order of 1. Like K2K, the initial flux is measured by a near detector, $L \sim 1$ km, and compared with the flux at the far detector to observe $\nu_\mu$ disappearance. Both detectors are based on magnetised steel and plastic scintillator (alternating planes) tracking calorimeters, of 1 kton targe mass (27 ton fiducial) for

the near detector and 5.4 kton (4.0 kton fiducial) for the far detector. The beam capability to switch between $\nu_\mu$ to $\bar{\nu}_\mu$ allows to measure oscillation parameters in case of $\bar{\nu}_\mu$ disappearance [22], and MINOS can also detect $\nu_e$ interaction through compact electromagnetic showers and attempts measurement of $\nu_\mu \rightarrow \nu_e$ oscillation, thus $\theta_{13}$ [23]. With an exposure of $7.25 \times 10^{20}$ protons on target, the ratio between the observed energy spectrum with the prediction without oscillation is shown in the bottom left plot of Fig. 2.8, where a clear sharp dip in the oscillation probability around 1 GeV, as expected by the SK results, is present. A fit to the data results in

$$|\Delta m^2_{32}| = 2.32^{+0.12}_{-0.08} \times 10^{-3}\ \text{eV}^2 \ \text{ and } \ \sin^2 2\theta_{23} > 0.90 \text{ at } 90\,\% \text{ C.L.} \qquad (2.21)$$

From the result in Eq. 2.18 together with the $\Delta m^2_{32}$ value of Eq. 2.21, it is noticed that $\Delta m^2_{21}$ is significantly smaller than $\Delta m^2_{32}$ and it is possible to make the approximation $\Delta m^2_{32} \approx \Delta m^2_{31}$, since there is the relation of Eq. 2.11.

Another attempt to explore neutrino oscillation using particle accelerators is the Oscillation Project with Emulsion-tRacking Apparatus (OPERA), installed at Italy's Laboratori Nazionali del Gran Sasso (LNGS). Instead of measuring oscillation parameters via $\nu_\mu$ disappearance, OPERA is designed to explicit detect $\nu_\tau$ appearance. Direct observation of $\nu_\tau$ would confirm the interpretation of SK results in terms of $\nu_\mu \rightarrow \nu_\tau$ oscillation. The $\nu_\mu$ beam, with a mean energy of about 17 GeV, is produced from a pulsed proton beam at CERN's Super Proton Synchrotron (SPS), about 730 Km from Gran Sasso. The $\tau$ lepton produced by $\nu_\tau$ charged current interaction is detected through the topology of its decay in nuclear emulsion films. The expected

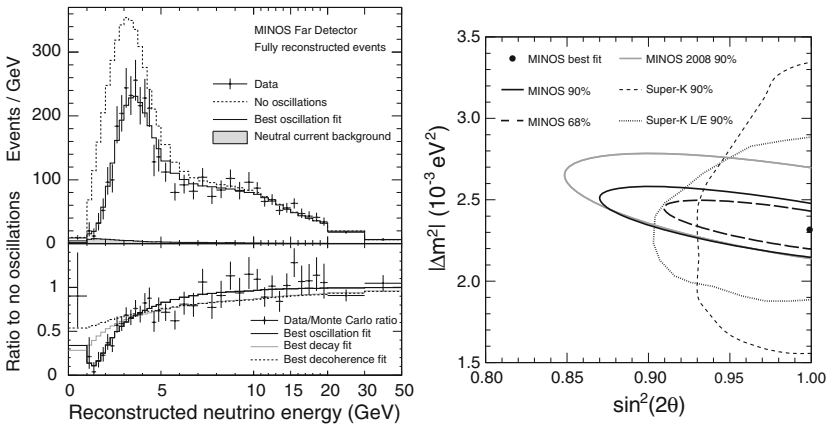


**Fig. 2.8** Results of $\nu_\mu$ disappearance in the MINOS experiment. The *left plot* shows the energy spectrum of fully reconstructed events in the far detector classified as CC interactions. The *dashed line* represents the spectrum predicted from the near detector assuming no ocillations, while the *solid histogram* reflects the best fit of the oscillation. The *right plot* shows the confidence level contours of 1 $\sigma$ and 90 %, around the oscillation parameters best fit values. Reprinted figure with permission from [24]

signal statistics is not very high, and only three $\nu_\tau$ have been observed (the absence of a signal from $\nu_\mu \rightarrow \nu_\tau$ oscillations is excluded at 3.4 $\sigma$) since data taking started in 2008 [25].

### 2.5.3 Measurement of $\theta_{13}$

The mixing angle $\theta_{13}$ is the smallest angle of the PMNS matrix. For this reason the related oscillations have been the most difficult to observe. While several experiments precisely measured the other two mixing angle, $\theta_{12}$ and $\theta_{23}$, only an upper limit of $\theta_{13}$ was given by the Chooz experiment [26], as $\sin^2 2\theta_{13} < 0.15$, not excluding a non oscillation scenario. The value of $\theta_{13}$ become accessible just recently, in mid-2011, thanks to the new generation of reactor and accelerator experiments, which provide sensitivities to small mixing angle of about one order of magnitude better than previous limits. Moreover reactor $\bar{\nu}_e$ experiments are complementary to long baseline accelerator experiments in determining $\theta_{13}$, since they are insensitive to the violation phase $\delta_{CP}$, and the dependence from the solar mass split is weak. Furthermore, over short baselines of about 1 Km the reactor $\bar{\nu}_e$ does not suffer from matter effects.

#### 2.5.3.1 By Accelerator Neutrinos

Long baseline accelerator experiments are designed to detect the appearance of $\nu_e$ from a $\nu_\mu$ beam with energy from few hundred MeV to few GeV, using far detectors at a few hundred km far from the neutrino source. This type of experiment has also sensitivity to the CP violation phase and the neutrino mass hierarchy. However, there are potentially parameter degeneracies leading to the following ambiguities:

- $\delta_{CP} - \theta_{13}$ ambiguity;
- sign of $\Delta m^2_{32}$ ambiguity;
- $\theta_{23}$ ambiguity.

In addition, accelerator experiments have to take into account matter effects on the neutrino oscillation, shortly described in Sect. 2.3, to determine the $\theta_{13}$ value.

As said in Sect. 2.5.2.2, the MINOS experiments can also perform a $\nu_e$ appearance measurement. With an exposure of $8.2 \times 10^{20}$ protons on target, the expected number of $\nu_e$ CC interactions on the far detector, based on the near detector data, was calculated to be $49.6 \pm 7.0(\text{stat.}) \pm (\text{sys.})$, assuming no oscillation, while 62 events were observed. Assuming $\delta_{CP} = 0$, $\Delta m^2_{32} = 2.32 \times 10^{-3}\,\text{eV}^2$ and normal (inverted) hierarchy, the upper limit of $\theta_{13}$, at a 90 % C.L., was set as $2 \sin^2 \theta_{23} \sin^2 2\theta_{13} < 0.12(0.20)$, while the $\theta_{13} = 0$ hypothesis is disfavoured by the data at the 89 % C.L.

The Tokai to Kamioka experiment (T2K) uses a muon neutrino beam produced at the Japan Proton Accelerator Research Complex (J-PARC), a segmented near detector ($L = 280\,\text{m}$) with a tracking system to precisely measure the non-oscillated flux and the well known SK detector in order to directly measure the appearance of $\nu_e$.

The $\nu_\mu$ beam is directed 2.5 degree away from the SK baseline of about 295 km. This off-axis configuration lower the neutrino flux but provide a narrow energy spectrum peaked at about 600 MeV. In summer 2011 T2K reported the observation of six $\nu_e$ in the SK detector, with an expected background level of $1.5 \pm 0.5$ events, providing a signal significance of about 2.5 $\sigma$ [27]. The T2K results have been updated in the beginning of 2013 with about more statistics and improved systematics uncertainty. A total of 11 $\nu_e$ events have been observed in the SK detector, with $3.3 \pm 0.4$ expected background events, as shown in Fig. 2.9. The background only hypothesis is rejected with a significance of 3.1 $\sigma$, and a fit, assuming $|\Delta m^2_{32}| = 2.4 \times 10^{-3}\,\text{eV}^2$, $\delta_{\text{CP}} = 0$, $\sin^2 2\theta_{23}$, and normal hierarchy, yields $\sin^2 2\theta_{13} = 0.088^{+0.049}_{-0.039}$.

#### 2.5.3.2 By Short Baseline Reactor Neutrinos

The new generation reactor experiments, Double Chooz, Daya Bay and RENO aim to measure $\theta_{13}$ by looking for distortion in the measured energy spectrum due to $\bar{\nu}_e$ disappearance, in a similar way KamLAND did for solar oscillation. Since the phase for $\theta_{13}$ oscillation is proportional to $\Delta m^2_{31} \simeq \Delta m^2_{32}$, about two order of magnitude bigger than the solar mass split, the baseline for $\theta_{13}$ measurements has to be of the order of 1 km, two order of magnitude smaller than KamLAND. The three reactor experiments are similar in concept and design, while differ mainly in the number of detectors and reactors and their relative positions. A near detector is used to compare its data with the far detector. In this way, the uncertainties related to the $\bar{\nu}_e$ flux and detection efficiencies can be largely suppressed. Details on the detector technology and $\bar{\nu}_e$ are exemplified in the next chapters, where the Double Chooz experiment is described in depth.

Daya Bay uses 6 detectors placed at different distances from 6 reactors, as shown in Fig. 2.10, and started the data taking in September of 2011. Each of its detectors has 20 tons of Gd loaded liquid scintillator and the reactors generates 2.9 $\text{W}_{\text{th}}$ each. They released their first result in early 2012 [29] using 55 days of data. This result was updated later using 139 days of data, giving a measurement of $\theta_{13}$ as follows

$$\sin^2 2\theta_{13} = 0.089 \pm 0.010(\text{stat.}) \pm 0.005(\text{syst.}), \tag{2.22}$$

assuming a three neutrino framework and rejecting $\theta_{13} = 0$ with a significance of 5.2 $\sigma$. More two detectors were installed in the year of 2013. Details of the Daya Bay analysis, which is based on the detectors' interaction rate, are given in Sect. 5.2.2.1.

RENO experiment uses two detectors, one near and one far from an array of 6 reactors, as shown in Fig. 2.11, and started the data taking in August of 2011. The detectors contains 16 ton of Gd loaded liquid scintillator, and with 229 days of data taking the collaboration also released their result on $\theta_{13}$ in early 2012. Based on the observed rate on their two detectors, a fit to the data yields

$$\sin^2 2\theta_{13} = 0.113 \pm 0.013(\text{stat.}) \pm 0.019(\text{syst.}), \tag{2.23}$$

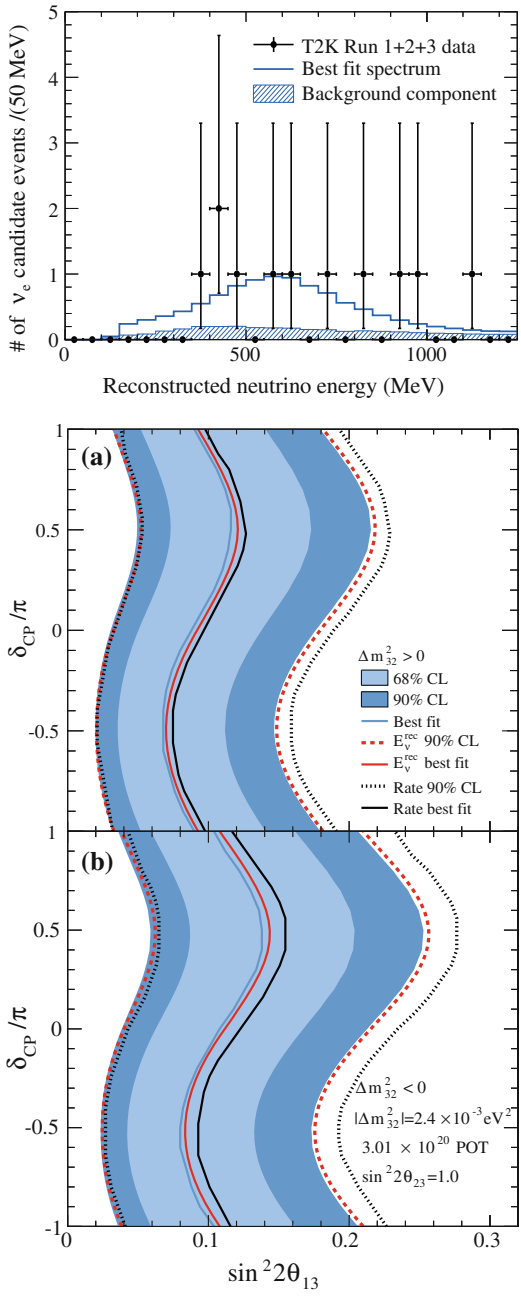


**Fig. 2.9** Results of the T2K experiment searching for $\nu_\mu \rightarrow \nu_e$ appearance. The *upper plot* shows the data and prediction reconstructed energy distribution, and the background expectation. The *solid line* represent the best fit spectrum assuming $\delta_{CP} = 0$ and normal hierarchy. The *bottom plot* shows the 68 and 90 % C.L. regions for $\sin^2 2\theta_{13}$ scanned over values of $\delta_{CP}$ assuming normal (*a*) or inverted (*b*) hierarchy. The best values of $\sin^2 2\theta_{13}$ for the energy spectrum and the rate analysis are also shown. Reprinted figure with permission from [28]

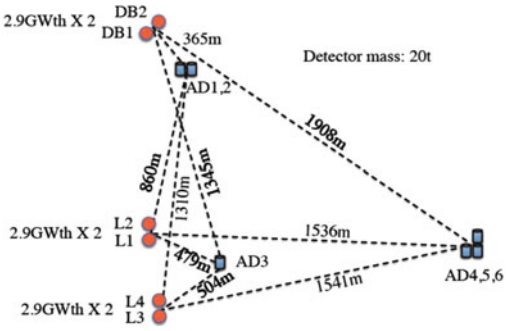


**Fig. 2.10** Relative locations of detectors and reactors of Daya Bay Experiment. Scale is approximate

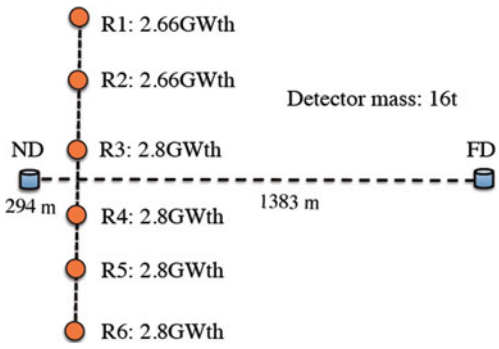


**Fig. 2.11** Relative locations of detectors and reactors of RENO. Scale is approximate

assuming a three neutrino framework and rejecting $\theta_{13} = 0$ with a significance of 4.9 $\sigma$. An updated result with more statistics and improved analysis will be released by the RENO collaboration soon.

The Double Chooz experiment, has its detector concept and design described in full detail in Chap. 3. The first result from reactor experiment was released by Double Chooz in November 2011 [30] and an updated analysis with major improvements with twice the statistics was released in July 2012 [31]. One objective of this work is to use the Double Chooz data in order to improve the $\theta_{13}$ measurement of

$$\sin^2 2\theta_{13} = 0.109 \pm 0.030(\text{stat.}) \pm 0.025(\text{sys.}), \tag{2.24}$$

using only a far detector, performing a new style of spectrum distortion analysis.

Finally, these new measurements of $\theta_{13}$ could provide further constrains on the measurements of $\Delta m^2_{21}$ and $\tan^2\theta_{12}$, by a three flavour oscillation analysis [18]. Although it does not change the central value and 1 $\sigma$ uncertainty of these parameters (Eq. 2.18), this constrain improves the significance of the result, making a narrower C.L. region, as it is possible to see in Fig. 2.12 when compared with Fig. 2.6.

The small, but non-zero, value of $\theta_{13}$ is a very good news for future neutrino programs for $\delta_{CP}$ measurement.

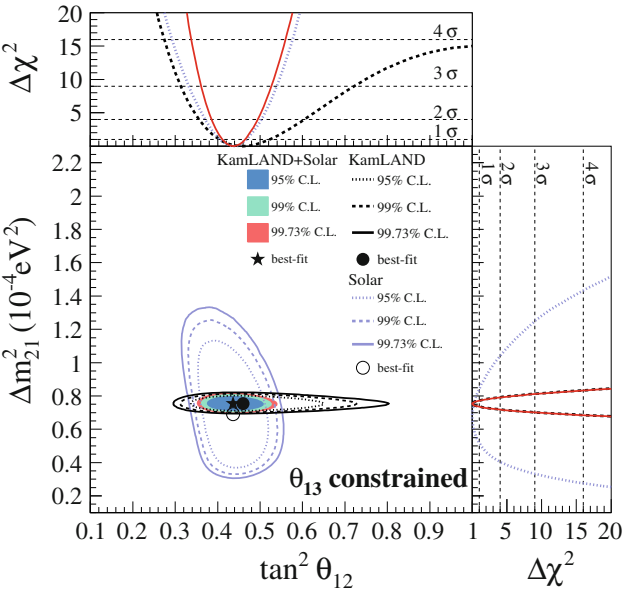


**Fig. 2.12** Allowed region for neutrino oscillation parameters from KamLAND and solar neutrino experiments when $\theta_{13}$ is constrained by reactor and accelerator experiments. Plot structure is the same as in Fig. 2.6. Reprinted figure with permission from [18]

### 2.5.4 Measurement of $\Delta m^2_{31}$

The mass squared difference $\Delta m^2_{31}$ can be measured by energy spectrum distortion and baseline dependence of the reactor-$\theta_{13}$ experiments. The neutrino oscillation probability going to the same flavour, expressed by Eq. 2.9, can be re-written in terms of the oscillation angles and squared mass difference, for $\bar{\nu}_e$, as follows

$$P(\overline{\nu}_e \to \overline{\nu}_e) = 1 - \sin^2 2\theta_{13}\left(c^2_{12}\sin^2\frac{\Delta m^2_{31}L}{4E} + s^2_{12}\sin^2\frac{\Delta m^2_{32}L}{4E}\right) + O(10^{-3}). \tag{2.25}$$

On the other hand, the survival probability of high energy $\nu_\mu$ which is produced by accelerator is,

$$P(\nu_\mu \to \nu_\mu) = 1 - \sin^2 2\theta_{23} \times \left(\begin{array}{c}(s^2_{12} + s_{13}t_{23}\sin 2\theta_{12}\cos\delta)\sin^2\frac{\Delta m^2_{31}L}{4E} \\ +(c^2_{12} - s_{13}t_{23}\sin 2\theta_{12}\cos\delta)\sin^2\frac{\Delta m^2_{32}L}{4E}\end{array}\right) + O(10^{-2}). \tag{2.26}$$

Usually oscillation data is analysed assuming two flavour oscillation formula,

$$P(\nu_\alpha \to \nu_\alpha) = 1 - \sin^2 2\theta \sin^2 \frac{\Delta\tilde{m}^2 L}{4E}, \tag{2.27}$$

and the measured mass square difference corresponds to a weighted mean of $\left|\Delta m^2_{32}\right|$ and $\left|\Delta m^2_{31}\right|$ [32],

$$\begin{aligned}\Delta\tilde{m}^2_{31} &= c^2_{12}\left|\Delta m^2_{31}\right| + s^2_{12}\left|\Delta m^2_{32}\right| \text{ and} \\ \Delta\tilde{m}^2_{32} &= (s^2_{12} + s_{13}t_{23}\sin 2\theta_{12}\cos\delta)\left|\Delta m^2_{31}\right| \\ &\quad + (c^2_{12} - s_{13}t_{23}\sin 2\theta_{12}\cos\delta)\left|\Delta m^2_{32}\right|,\end{aligned} \tag{2.28}$$

where $t_{ij} = \tan\theta_{ij}$. They are called effective $\Delta m^2$. Note that $\Delta\tilde{m}^2$ is not a difference of the mass square and is positive definite. Since there is a relation

$$\Delta m^2_{31} = \Delta m^2_{32} + \Delta m^2_{21}, \tag{2.29}$$

in the standard three-flavor scheme, the difference between $\Delta\tilde{m}^2_{31}$ and $\Delta\tilde{m}^2_{32}$ is expressed as follows

$$\begin{aligned}\frac{2(\Delta\tilde{m}^2_{31} - \Delta\tilde{m}^2_{32})}{\Delta\tilde{m}^2_{31} + \Delta\tilde{m}^2_{32}} &\sim \pm(1 - s_{13}t_{23}\tan 2\theta_{12}\cos\delta) \times \frac{2\cos 2\theta_{12}|\Delta m^2_{21}|}{|\Delta m^2_{31}| + |\Delta m^2_{32}|} \\ &\sim \pm 0.012 \times (1 \pm 0.3),\end{aligned} \tag{2.30}$$

where the overall sign depends on mass hierarchy, and the $\pm 0.3$ term comes from the ambiguity of $\cos\delta$. If $\Delta\tilde{m}^2_{31} > \Delta\tilde{m}^2_{32}$, it is normal hierarchy, and vise versa.

In order to distinguish the mass hierarchy cases, it is necessary to distinguish the separation of 1.7–3.1 % depending on $\delta$. $\Delta\tilde{m}^2_{32}$ has been measured with precision of $\sim$3.5 % [33]. So far there has been no reported measurement of $\Delta\tilde{m}^2_{31}$ and this work proposes to measure it for the first time. If the difference between $\Delta\tilde{m}^2_{31}$ and $\Delta\tilde{m}^2_{32}$ is larger than 1.6 %, it can not be explained by the standard three flavour oscillation scheme. If both $\Delta\tilde{m}^2_{31}$ and $\Delta\tilde{m}^2_{32}$ are measured with a 1 % accuracy or better in the future, the mass hierarchy and $\cos\delta$ can be measured.

## 2.6 Neutrino Mass

As highlighted in Sect. 2.1, $\mathscr{SM}$ neutrinos are not allowed to acquire masses through the Higgs mechanism because they exist only in the left-handed chiral state (right-handed for anti-neutrinos). However, experimental evidence of neutrino oscillations imply the neutrino must be a massive particles. Further hints of a non-null neutrino mass can be investigated independently from neutrino oscillation. In particular, experiments looking for distortion induced by massive neutrinos on the beta decay end

point of tritium, $^3\mathrm{H} \rightarrow {}^3\mathrm{He} + e^- + \bar{\nu}_e$, set a limit $\bar{\nu}_e$ mass below 2 eV [34]. Similarly, the observation of the cosmic microwave background and the density fluctuations, and other cosmological measurements, put a combined upper limit on neutrino mass around 0.5 eV [35], which is six orders of magnitude smaller than the electron mass.

Given the evidences of neutrinos being massive particles, it is necessary to extend the $\mathscr{SM}$ to include neutrino masses. The most simple extension of the $\mathscr{SM}$ is to add a right-handed neutrino singlet. In this case, neutrino masses are acquired through the Higgs mechanism, like all other fermions:

$$\mathscr{L}_D \simeq -m_D \bar{\nu}_L \nu_R + h.c. \tag{2.31}$$

$m_D$ is the so called Dirac mass term and has the same form of the fermion masses in Eq. 2.3:

$$m_\nu = \frac{v}{\sqrt{2}} \Gamma_\nu. \tag{2.32}$$

With this model the Yukawa coupling constant $\Gamma_\nu \simeq m_\nu / v$ needs to be of the order of $10^{-12}$, which is far too small compared to the other fermions ($\Gamma_e \simeq 0.3 \times 10^{-5}$) and it is commonly considered as unnatural.

Since neutrinos do not have electromagnetic charge, they could be described in term of a Majorana particles:

$$\nu^c = C \bar{\nu}^T \equiv \nu, \tag{2.33}$$

where $\nu^c = C\bar{\nu}^T$ is the charge conjugate of the field $\nu^c$, and $C$ is the charge conjugation. Considering a left-handed Majorana particle, $\nu = \nu_L + \nu_L^c$, a Majorana mass term of the form:

$$\mathscr{L}_D \simeq -m_M \bar{\nu^c}_L \nu_L + h.c. \tag{2.34}$$

could be considered. It should be noted that the Majorana mass term involves left-handed neutrino only and is not gauge invariant, $m\bar{\nu^c}\nu \rightarrow m\bar{\nu^c} e^{i2\alpha}\nu$, violating lepton flavour number by two units.

The smallness of the neutrino mass term is no longer dependent on the unnatural Yukawa coupling constant, but nonetheless a mass term for a left-handed neutrino is not allowed by the $\mathscr{SM}$ because it implies an Higgs triplet with isospin one.

Once a right-handed neutrino is introduced to obtain a Dirac mass term, a Majorana mass term could also be obtained in case the right-handed neutrino is Majorana particle. The most general mass term can thus be written as mix of Dirac and Majorana term:

$$\begin{aligned} \mathscr{L}_{D+M} &= \mathscr{L}_D + \mathscr{L}_{M_R} + \mathscr{L}_{M_L} \\ &= -m_D \bar{\nu}_L \nu_R - m_{M_R} \bar{\nu^c}_R \nu_R - m_{M_L} \bar{\nu^c}_L \nu_L + h.c. \end{aligned} \tag{2.35}$$

which can be written as

$$\mathscr{L}_{D+M} = -\frac{1}{2}\left(\bar{\nu^c}_L \;\; \bar{\nu}_R\right)\begin{pmatrix} m_L & m_D \\ -m_D & m_R \end{pmatrix}\begin{pmatrix} \nu_L \\ \bar{\nu}_R \end{pmatrix} + h.c. \tag{2.36}$$

The term $m_L$ is the left-handed neutrino Majorana mass, $m_R$ is the right-handed neutrino Majorana mass and $m_D$ is the Dirac mass. The mass matrix can be diagonalised in term of the mass eigenstate:

$$\nu_L = \cos\theta\nu_1 + \sin\theta\nu_2 \tag{2.37}$$

$$\nu_R^c = -\sin\theta\nu_1 + \cos\theta\nu_2 \tag{2.38}$$

with eigenstate $m_{1,2}$

$$m_{1,2} = \frac{1}{2}\left(m_L + m_R \pm \sqrt{(m_L - m_R)^2 + m_D^2}\right) \tag{2.39}$$

and

$$\tan 2\theta = \frac{2m_D}{m_R - m_L}. \tag{2.40}$$

Since the left handed Majorana mass term requires an Higgs triplet, in the minimal $\mathscr{SM}$ extension, $m_L$ is usually set to zero. The right-handed Majorana neutrino is an electroweak singlet acquiring a mass independently from the Yukawa coupling. In the limit where $m_L = 0$ and $m_R \gg m_D$:

$$\tan 2\theta \simeq \frac{2m_D}{m_R} \simeq 0,\; m_1 \simeq \frac{m_D^2}{m_R} \text{ and } m_2 \simeq m_R, \tag{2.41}$$

with one light left-handed neutrino and one heavy right-handed neutrino:

$$\nu_1 \simeq (\nu_L - \nu_L^c), \tag{2.42}$$

$$\nu_2 \simeq (\nu_R + \nu_R^c). \tag{2.43}$$

This is the so called see-saw mechanism, which involves two Majorana particles: a very heavy right-handed neutrino and the observed light left-handed neutrino. The smallness of the observed neutrino mass could then be explained in terms of a Dirac mass of the order of the electroweak energy scale, without the unnatural Yukawa coupling constant, and a much bigger Majorana mass term. The term $m_R$ is generally related to the grand unification scale around the Planck scale at $10^{16}$ eV.

The Dirac or Majorana nature of the neutrino is not yet known. Experimentally it is possible to investigate this question through processes violating the lepton number like the neutrino-less double beta decay, which violates the lepton quantum number by two units. Many experiment are currently, or will soon, searching the neutrino-less

double beta decay, CUORE [36], GERDA [37], EXO [38] and SUPER-NEMO [39], but no signal has been observed up to now.

## 2.7 Neutrino Anomalies

So far neutrino oscillation is well established in terms of a three flavour framework. However, there are some experiments whose results are not explained by this framework and might require the introduction of an extra sterile neutrino, i.e., a neutrino not participating in the $\mathscr{SM}$ interactions.

The first evidence of more than three neutrino flavours came from the Liquid Scintillator Neutrino Detector (LSND) experiment [40]. Using a $\bar{\nu}_\mu$ from pion decay detected in a liquid scintillator, LSND found $>3\,\sigma$ evidence of $\bar{\nu}_\mu \rightarrow \bar{\nu}_e$ transition which would require a mass splitting of about $0.2\,\mathrm{eV}^2$, larger than the atmospheric one. The LSND anomaly has been tested by the Fermilab's MiniBooNE (Mini Booster Neutrino Experiment) in both neutrino and antineutrino mode. The results obtained in the neutrino mode disfavour most of the parameter space defined by LSND but were not conclusive [41]. The results obtained in the antineutrino mode instead were consistent with LSND signal and consistent with a mass split of between 0.1 and $1\,\mathrm{eV}^2$ [42]. Further hints of the existence of sterile neutrinos came from measurements of neutrino fluxes from intense radioactive sources in the GALLEX [43] and SAGE [44] detectors. An unexpected reduction of the $\nu_e$ flux consistent with $\nu_e$ disappearance has been found at $2.7\,\sigma$. The interpretation in terms of sterile neutrino oscillation indicates a value for the squared mass difference of about $0.35\,\mathrm{eV}^2$.

Recent re-evaluation of the expected antineutrino flux from nuclear reactor indicates that the measured flux is about 6 % below the prediction with $3\,\sigma$ significance, as shown in Fig. 2.13. Even if such a deficit could still be due to some unknown effects in the reactor neutrino production or a non accurate knowledge of the fission product contribution to the antineutrino spectrum, it is consistent with $\bar{\nu}_e$ flux suppression due to sterile neutrino oscillation with mass split of about $2.4\,\mathrm{eV}^2$.

In summary, there are hints compatible with the existence of sterile neutrinos from several experiments, using different sources and detection technique, but none of them could claim a discovery. Many experiments have been proposed for sterile neutrino search and an exhaustive list can be found in [46].

## 2.8 Summary and Open Questions

Over the last twenty years many experimental efforts have provided clear confirmation that neutrinos are massive particle and that there is mixing between flavour and mass eigenstates. The solar neutrino anomaly has been solved by SNO and KamLAND experiments, and the missing solar neutrino flux is interpreted within the neutrino oscillation scenario, of three neutrino flavours. Atmospheric neutrino

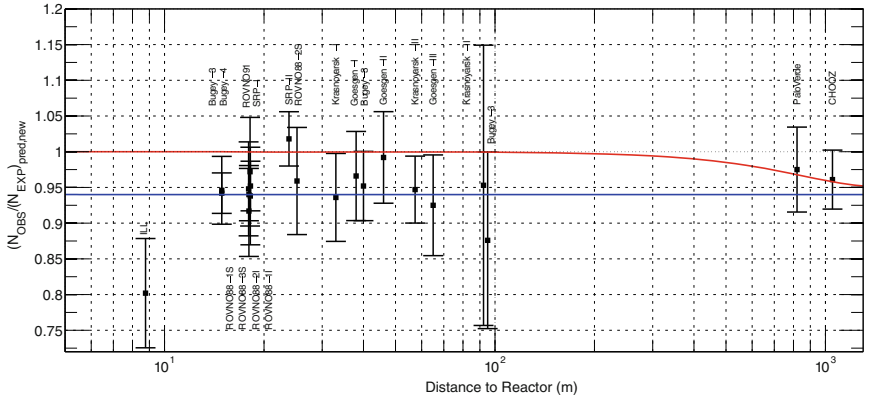


**Fig. 2.13** Illustration of the short baseline reactor antineutrino anomaly. The experimental results are compared to the prediction without oscillation, taking into account the new antineutrino spectra, the corrections of the neutron mean lifetime, and the off-equilibrium effects. The *red line* shows a possible 3 active neutrino mixing solution, with $\sin^2 2\theta_{13} = 0.06$. The *blue line* displays a solution including a new neutrino mass state, such as $|\Delta m^2_{\text{new}}| \gg 1\,\text{eV}^2$ and $\sin^2 2\theta_{\text{new}} = 0.12$, for illustration purpose. Reprinted figure with permission from [45]

oscillations has been characterised by SK and K2K and MINOS long baseline accelerator experiments. The observed disappearance of atmospheric neutrinos also has been interpreted in terms of oscillations. The latest mixing angle, $\theta_{13}$ was finally measured by reactor and accelerator experiments, and it is currently under precision determination era.

With the current characterisation of the PMNS matrix, new measurements will be possible in order to improve the current knowledge and to complete neutrino oscillation picture concerning the still open questions:

- Which is the value of the CP-violating phase, $\delta_{CP}$? It can be measured in long baseline experiments, studying the oscillation probability asymmetries between neutrino and antineutrinos.
- What is the neutrino mass hierarchy? The matter effect could be used in long baseline experiments to measure the sign of $\Delta m^2_{32}$ and establish the neutrino mass hierarchy. This also can be done by reactor experiments with a baseline of $\sim$50 km.
- What is the sign of $\cos 2\theta_{23}$? By the combination of reactor $\bar{\nu}_e$ and both accelerator $\nu_\mu$ disappearance and $\nu_e$ appearance. The degeneracy on the measurement of $\theta_{23}$ at accelerator experiment will be broken by the reactor $\theta_{13}$ measurement which does not depend on the first. Therefore, a discrimination of the fraction of $\nu_\mu$ and $\nu_\tau$ contained by the mass state $\nu_3$ will be possible to be performed.

Beyond neutrino oscillations, neutrinos absolute mass scale determination, their Dirac or Majorana nature understanding, and the confirmation or not of the existence of a fourth sterile neutrino, are also current challenges for the neutrino physics community.

## References


1. G. Aad et al. (ATLAS Collaboration), Observation of a new particle in the search for the standard model Higgs Boson with the ATLAS detector at the LHC. Phys. Lett. B **716**(1), 1–29 (2012)
2. B. Pontecorvo, Mesonium and anti-mesonium. Sov. Phys. JETP **6**, 429 (1957)
3. Z. Maki, M. Nakagawa, S. Sakata, Remarks on the unified model of elementary particles. Prog. Theor. Phys. **28**(5), 870–880 (1962)
4. S.P. Mikheev, A.Yu. Smirnov, Resonance amplification of oscillations in matter and spectroscopy of solar neutrinos. Sov. J. Nucl. Phys. **42**, 913–917 (1985)
5. L. Wolfenstein, Neutrino oscillations in matter. Phys. Rev. D **17**, 2369–2374 (1978)
6. A. De Rújula, M.B. Gavela, P. Hernández, Atmospheric neutrino anomaly without maximal mixing? Phys. Rev. D **63**, 033001 (2001)
7. B. Richter, Conventional beams or neutrino factories: the next generation of accelerator based neutrino experiments (2000), arXiv:hep-ph/0008222
8. H. Nunokawa, S. Parke, R.Z. Funchal, What fraction of Boron-8 solar neutrinos arrive at the Earth as a $\nu_2$ mass eigenstate? Phys. Rev. D **74**, 013006 (2006)
9. J.N. Bahcall, A.M. Serenelli, S. Basu, New solar opacities, abundances, helioseismology, and neutrinofluxes. Astrophys. J. Lett. **621**(1), L85 (2005). Copyright (2014) by the American Astronomical Society
10. R. Davis, D.S. Harmer, K.C. Hoffman, Search for neutrinos from the Sun. Phys. Rev. Lett. **20**, 1205–1209 (1968)
11. W. Hampel et al. (GALLEX Collaboration), GALLEX solar neutrino observations: results for GALLEX IV. Phys. Lett. B **447**(12), 127–133 (1999)
12. M. Altmann et al. (GNO Collaboration), GNO solar neutrino observations: results for GNO I. Phys. Lett. B **490**(12), 16–26 (2000)
13. J.N. Abdurashitov et al. (SAGE Collaboration), Results from SAGE (The Russian-American gallium solar neutrino experiment). Phys. Lett. B **328**(12), 234–248 (1994)
14. Y. Fukuda et al. (Super-Kamiokande Collaboration), Measurements of the solar neutrino flux from Super-Kamiokande's first 300 days. Phys. Rev. Lett. **81**, 1158–1162 (1998)
15. B. Aharmim et al. (SNO Collaboration), Electron energy spectra, fluxes, and day-night asymmetries of $^8$B solar neutrinos from measurements with NaCl dissolved in the heavy-water detector at the Sudbury Neutrino Observatory. Phys. Rev. C **72**, 055502 (2005)
16. B. Aharmim et al. (SNO Collaboration), Determination of the $\nu_e$ and total $^8$B solar neutrino fluxes using the Sudbury Neutrino Observatory phase I data set. Phys. Rev. C **75**, 045502 (2007). Copyright (2014) by the American Physical Society
17. S. Abe et al. (KamLAND Collaboration), Precision measurement of neutrino oscillation parameters with KamLAND. Phys. Rev. Lett. **100**, 221803 (2008). Copyright (2014) by the American Physical Society
18. A. Gando et al. (KamLAND Collaboration), Reactor on-off antineutrino measurement with KamLAND. Phys. Rev. D **88**, 033001 (2013). Copyright (2014) by the American Physical Society
19. Y. Ashie et al. (Super-Kamiokande Collaboration), Evidence for an oscillatory signature in atmospheric neutrino oscillations. Phys. Rev. Lett. **93**, 101801 (2004). Copyright (2014) by the American Physical Society
20. J. Hosaka et al. (Super-Kamiokande Collaboration), Three flavor neutrino oscillation analysis of atmospheric neutrinos in super-kamiokande. Phys. Rev. D **74**, 032002 (2006). Copyright (2014) by the American Physical Society
21. M.H. Ahn et al. (K2K Collaboration), Measurement of neutrino oscillation by the K2K experiment. Phys. Rev. D **74**, 072003 (2006)
22. P. Adamson et al. (MINOS Collaboration), Search for the disappearance of muon antineutrinos in the NuMI neutrino beam. Phys. Rev. D **84**, 071103 (2011)
23. P. Adamson et al. (MINOS Collaboration), Improved search for muon-neutrino to electron-neutrino oscillations in MINOS. Phys. Rev. Lett. **107**, 181802 (2011)

24. P. Adamson et al. (MINOS Collaboration), Measurement of the neutrino mass splitting and flavor mixing by MINOS. Phys. Rev. Lett. **106**, 181801 (2011). Copyright (2014) by the American Physical Society
25. N. Agafonova et al. (OPERA Collaboration), Evidence for $\nu_\mu \rightarrow \nu_\tau$ appearance in the CNGS neutrino beam with the OPERA experiment. Phys. Rev. D **89**, 051102 (2014)
26. M. Apollonio et al. (CHOOZ Collaboration), Search for neutrino oscillations on a long baseline at the Chooz nuclear power station. Eur. Phys. J. **C27**, 331–374 (2003)
27. K. Abe et al. (T2K Collaboration), Indication of electron neutrino appearance from an accelerator-produced off-axis muon neutrino beam. Phys. Rev. Lett. **107**, 041801 (2011)
28. K. Abe et al. (T2K Collaboration), Evidence of electron neutrino appearance in a muon neutrino beam. Phys. Rev. D **88**, 032002 (2013). Copyright (2014) by the American Physical Society
29. F.P. An et al. (Daya Bay Collaboration), Observation of electron-antineutrino disappearance at Daya Bay. Phys. Rev. Lett. **108**, 171803 (2012)
30. Y. Abe et al. (Double Chooz Collaboration), Indication of reactor $\overline{\nu}_e$ disappearance in the Double Chooz experiment. Phys. Rev. Lett. **108**, 131801 (2012)
31. Y. Abe et al. (Double Chooz Collaboration), Reactor $\overline{\nu}_e$ disappearance in the Double Chooz experiment. Phys. Rev. D **86**, 052008 (2012)
32. H. Nunokawa, S. Parke, R.Z. Funchal, Another possible way to determine the neutrino mass hierarchy. Phys. Rev. D **72**, 013009 (2005)
33. G.L. Fogli, Invited talk on 'Global analysis of neutrino oscillations', in *The XXV International Conference on Neutrino Physics and Astrophysics* (*Neutrino 2012*), Kyoto, 2012, http://neu2012.kek.jp/
34. J. Beringer et al. (Particle Data Group), Review of particle physics. Phys. Rev. D **86**, 010001 (2012)
35. K. Nakamura et al. (Particle Data Group), Review of particle physics. J. Phys. G: Nucl. Part. Phys. **37**(7A), 075021 (2010)
36. C. Arnaboldi et al. (CUORE Collaboration), Results from a search for the 0 $\nu\beta\beta$-decay of $^{130}$Te. Phys. Rev. C **78**, 035502 (2008)
37. I. Abt et al. (GERDA Collaboration), A new Ge-76 double beta decay experiment at LNGS: letter of intent (2004), arXiv:hep-ex/0404039
38. M. Danilov et al. (EXO Collaboration), Detection of very small neutrino masses in double-beta decay using laser tagging. Phys. Lett. B **480**(12), 12–18 (2000)
39. F. Piquemal, The SuperNEMO project. Phys. At. Nucl. **69**(12), 2096–2100 (2006)
40. A. Aguilar et al. (LSND Collaboration), Evidence for neutrino oscillations from the observation of $\overline{\nu}_e$ appearance in a $\overline{\nu}_\mu$ beam. Phys. Rev. D **64**, 112007 (2001)
41. A.A. Aguilar-Arevalo et al. (MiniBooNE Collaboration), Unexplained excess of electronlike events from a 1 GeV neutrino beam. Phys. Rev. Lett. **102**, 101802 (2009)
42. A.A. Aguilar-Arevalo et al. (MiniBooNE Collaboration), Event excess in the MiniBooNE search for $\overline{\nu}_\mu \rightarrow \overline{\nu}_e$ oscillations. Phys. Rev. Lett. **105**, 181801 (2010). Copyright (2014) by the American Physical Society
43. W. Hampel et al. (GALLEX Collaboration), Final results of the $^{51}$Cr neutrino source experiments in GALLEX. Phys. Lett. B **420**(12), 114–126 (1998)
44. J.N. Abdurashitov et al. (SAGE Collaboration), Measurement of the response of a Ga solar neutrino experiment to neutrinos from a $^{37}$Ar source. Phys. Rev. C **73**, 045805 (2006)
45. G. Mention, M. Fechner, Th. Lasserre, Th.A. Mueller, D. Lhuillier, M. Cribier, A. Letourneau, Reactor antineutrino anomaly. Phys. Rev. D **83**, 073006 (2011). Copyright (2014) by the American Physical Society
46. K.N. Abazajian et al., Light sterile neutrinos: a white paper (2012), arXiv:1204.5379 [hep-ph]

http://www.springer.com/978-4-431-55374-8

Double Chooz and Reactor Neutrino Oscillation θ_13 Improvement and First Effective Δm^2_31 Measurement

Junqueira de Castro Bezerra, T.

2015, XVIII, 190 p. 144 illus., 46 illus. in color.,
Hardcover
ISBN: 978-4-431-55374-8